Irf8 regulates macrophage versus neutrophil fate during zebrafish primitive myelopoiesis

Li Li,[1] Hao Jin,[1] Jin Xu,[1] Yuqian Shi,[1] and Zilong Wen[1]

[1]State Key Laboratory of Molecular Neuroscience, Department of Biochemistry, Hong Kong University of Science and Technology, Clear Water Bay, Kowloon, Hong Kong, People's Republic of China

In vertebrates, myeloid cells comprise polymorphonuclear and mononuclear lineages that arise from 2 successive waves of development: a transitory primitive wave giving rise to limited myeloid cells during embryonic stage and a definitive wave capable of producing myeloid cells throughout the fetal and adult life. One key unresolved question is what factors dictate polymorphonuclear versus mononuclear lineage fates during myelopoiesis. Here we show that during zebrafish embryogenesis interferon regulatory factor-8 (*irf8*) is expressed specifically in macrophages but not neutrophils. Suppression of Irf8 function in zebrafish causes a depletion of macrophages and an enhanced output of neutrophils but does not affect the overall number, proliferation, and survival of primitive myeloid cells. These data indicate that the skewed myeloid lineage development in Irf8 knockdown embryos results from a cell-fate switching. Such a conclusion is further supported by the observation showing that overexpression of Irf8 promotes macrophage formation at the expense of neutrophil development. Genetic epistasis analysis reveals that Irf8 acts downstream of Pu.1 but is insufficient to promote macrophage development in the absence of Pu.1. Our findings demonstrate that Irf8 is a critical determinant for neutrophil versus macrophage fate choice during zebrafish primitive myelopoiesis. (*Blood*. 2011;117(4):1359-1369)

Introduction

Myeloid cells or phagocytes are a subtype of leukocytes that play essential roles in the host defense, embryogenesis, organogenesis, and tissue regeneration.[1-3] In vertebrates, myeloid cells are classified into 2 major lineages: polymorphonuclear and mononuclear lineages, which acquire different morphologies during development and exert overlapping but distinctive biologic functions. Polymorphonuclear phagocytes consist of neutrophils, eosinophils, basophils, and mast cells. They are the key effectors of inflammatory response on pathogen infection and tissue injury. On the other hand, mononuclear phagocytes, which include circulating macrophages, dendritic cells, and tissue-resident macrophages (osteoclasts in the bone, microglia in the brain, and Kupffer cells in the liver), not only play important roles in inflammatory response but also participate in organogenesis and tissue regeneration.[2,3] Despite differences in morphology and biologic function, polymorphonuclear and mononuclear phagocytes are thought to derive from a common myeloid-restricted population termed neutrophil-macrophage progenitors.[4] These multipotent neutrophil-macrophage progenitors then differentiate to macrophage-dendritic cell progenitors, neutrophil-macrophage progenitors, and basophil-mast cell bipotent progenitors, which in turn undergo terminal differentiation to produce mature dentritic cells, macrophages, neutrophils, basophils, and mast cells.[5] This developmental process is tightly controlled, and dysregulation of phagocyte development and function is associated with several human diseases, including cancer, autoimmune disorders, and neurodegenerative disorders.

Interferon regulatory factor-8 (IRF8), also known as the interferon consensus sequence-binding protein, was first identified through screening mouse λ expression libraries with interferon consensus sequence as a probe.[6] It encodes a transcription factor of IRF family, which contains a highly conserved N-terminal DNA-binding domain and a less conserved C-terminal IRF association domain.[7] Among the 9 members of the mammalian IRF family, IRF4 and IRF8 share the highest similarity in protein sequence and they are predominantly expressed in lymphocytes, macrophages, and dendritic cells.[8] The importance of IRF8 in hematopoiesis is first revealed by genetic studies in IRF8 knockout (IRF8-null)[9] and BXH-2 mutant mice, which carry a loss-of-function mutation in the IRF association domain of IRF8 protein.[10] Both IRF8-null and BXH-2 mutant mice have chronic myeloid leukemia with a profound increase of neutrophil number.[9,10] In addition, loss-of-function mutation in *IRF8* gene in these animals also causes a severe reduction of macrophages and dendritic cells.[10-13] These in vivo studies reveal that IRF8 is essential for myeloid progenitor differentiation toward macrophages but is dispensable for neutrophil development during adult murine myelopoiesis. Subsequent study shows that forced expression of IRF8 in IRF8-deficient myeloid progenitor cell line promotes macrophage differentiation and suppresses neutrophil development.[14] This in vitro observation suggests that IRF8 may serve as an intrinsic cell-fate determinant for macrophages versus neutrophils. However, in vivo evidence supporting such a conclusion is still lacking. Moreover, whether IRF8 plays a similar role during primitive myelopoiesis, which has a distinct origin from definitive myelopoiesis,[15,16] remains unexplored.

Here we provide in vivo evidence demonstrating that, during zebrafish primitive myelopoiesis, Irf8 is a critical determinant for macrophage versus neutrophil fate choice. Expression of Irf8

Submitted June 14, 2010; accepted October 28, 2010. Prepublished online as *Blood* First Edition paper, November 15, 2010; DOI 10.1182/blood-2010-06-290700.

The online version of this article contains a data supplement.

The publication costs of this article were defrayed in part by page charge payment. Therefore, and solely to indicate this fact, this article is hereby marked "advertisement" in accordance with 18 USC section 1734.

promotes the formation of macrophages and suppresses that of neutrophils. We further reveal that Irf8 acts downstream of Pu.1 but is insufficient to direct the formation of macrophages on loss of Pu.1 activity.

Methods

Fish lines

AB and Tg(mpx:eGFP)[17] fish strains were used in this study.

In vitro synthesis of antisense RNA probe

Antisense RNA probes were prepared by in vitro transcription according to the standard protocol. The following digoxigenin-labeled antisense probes were used: *irf8*, *csf1r*, *mpx*, *cebp1, lyz*, *pu.1, lcp1*, and *apoeb*.

Single- and 2-color WISH

Single-color whole-mount in situ hybridization (WISH) was performed as described.[18] The procedure of 2-color fluorescence in situ hybridization was reported previously.[19]

Single and double fluorescence immunohistochemistry staining

Immunohistochemistry was performed essentially as described previously.[19] To examine the costaining of green fluorescent protein (GFP) and DsRed, the embryos were first stained with goat anti-GFP and rabbit anti–DsRed antibody (1:250, 4°C, overnight) and were subsequently visualized by AlexaFluor-488 donkey anti–goat (1:400, 4°C, overnight) for GFP and AlexaFluor-555 donkey anti–rabbit for DsRed (1:400, 4°C, overnight). A similar procedure was used for costaining of GFP and Lcp1 protein.[19] AntiLcp1 antibody was visualized by AlexaFluor donkey anti–rabbit 647 (1:400, 4°C, overnight; Invitrogen).

Double staining for RNA (*csf1r* and *irf8*) and protein (Lcp1 and GFP)

WISH staining (*csf1r* or *irf8*) was first developed with Cy3 tyramide (PerkinElmer Life and Analytical Sciences). Afterward, embryos were washed with phosphate-buffered saline with Tween-20 for 6 × 20 minutes/each at room temperature. The embryos were then incubated with anti-Lcp1 or anti-GFP antibody (1:250 dilution, 4°C, overnight) and visualized by AlexaFluor-647 donkey anti–rabbit or AlexaFluor-488 donkey anti–goat (1:400, 4°C, overnight).

BrdU labeling and triple staining

Bromodeoxyuridine (BrdU) labeling was performed as described.[20] For Lcp1, GFP, and pH3 triple staining, Tg(*mpx*:eGFP) embryos were collected at 32 hours post-fertilization (hpf) and fixed in 4% paraformaldehyde. The fixed embryos were incubated with primary rabbit anti–phospho-histone H3 (pH3; Upstate Biotechnology) and goat anti-GFP (Abcam) antibodies according to the manufacturer's protocol and subsequently stained with AlexaFluor-647 anti–rabbit and AlexaFluor-488 anti–goat secondary antibodies (Invitrogen). After extensive washing, the embryos were stained with chicken anti-Lcp1 antibody and horseradish peroxidase-conjugated antichicken secondary antibody followed by detection with Cy3 tyramide.

SB staining

Sudan black (SB; Sigma-Aldrich) solution was used to treat the fixed embryos as described.[21] The SB-stained embryos were then washed by 70% ethanol, and signals were observed under microscope.

DIC imaging

Video-enhanced differential interference contrast (DIC) microscopy was performed on a Nikon 90i (60× water-immersion objective) microscope as reported.[21] Live specimens were anesthetized with tricaine in embryo medium and observed in depression slides.

Generation of *Tg(hsp70*:Irf8^{myc}) transgenic line and overexpression assay

The heat shock inducible Myc-tagged Irf8 (Irf8^{myc}) was constructed by inserting the N-terminal Myc-tagged Irf8 into the pTal vector under the control of the heat shock protein 70 (*hsp70*) promoter.[22] The construct was injected to one-cell stage embryos, and the injected embryos were raised to adult (F0). Tg(*hsp70*:Irf8^{myc}) founders were identified by examining the *hsp70-irf8^{myc}* DNA and Myc-tagged Irf8 (anti-Myc antibody staining). The stable F1 Tg(*hsp70*:Irf8^{myc}) fish were finally generated by mating the founder line with wild-type (WT) AB. Heat shock treatment was carried out with 11 hpf F2 embryos at 39.5°C for 1.5 hours.

Phagocytosis assays

Escherichia coli cells engineered with DsRed[23] were grown in *kana*$^+$ medium at 37°C for 2 days. Bacteria were harvested and suspended in phosphate-buffered saline to the concentration OD600 = 2.08. Approximately 2 nL of bacterial suspension was microinjected into the circulation of each anesthetized 40 hpf Tg(*mpx*:eGFP) and Tg(*hsp70*:Irf8^{myc}) embryo. At 30 minutes after injection, images were taken by Carl Zeiss LSM 510 confocal (40×).

MO

irf8 morpholino oligonucleotides (MO)^{sp} (5′-AATGTTTCGCTTACTTTGAAAATGG-3′), *irf8* MO^{atg} (5′-TCAGTCTGCGACCGCCCGAGTTCAT-3′), and *pu.1* MO (5′-AATAACTGATACAAACTCACCGTTC-3′) were designed based on *irf8* and *pu.1* gene sequence (http://www.ensembl.org/Danio_rerio/Info/Index). Standard control morpholino was purchased from Gene Tools. One-cell stage embryos were injected with 2 nL of morpholino solution at a concentration of 0.6mM *irf8* MO^{sp}, 0.3mM *irf8* MO^{atg}, or 0.5mM *pu.1* MO.

DsRed reporter assay

To assay the effectiveness of *irf8* MO^{atg}, a 267-bp *irf8* cDNA fragment (27 bp upstream and 240 bp downstream of ATG start site) was fused with DsRed cDNA and cloned into PCS2+ vector. This *irf8*-DsRed reporter construct, which contains the *irf8* MO^{atg} target site, was injected to one-cell stage WT embryos together with or without *irf8* MO^{atg}. DsRed was determined by fluorescent microscope at 24 hours after injection.

RT-PCR

Semiquantitative reverse-transcribed polymerase chain reaction (RT-PCR) was carried out with total RNA isolated from 18 hpf *irf8* MO^{sp} morphants or control embryos. *ef1a* and *pu.1* were amplified by 16 and 25 cycles, respectively (94°C for 30 seconds; 60°C for 30 seconds; 72°C for 40 seconds). The primers used for PCR were: *irf8*, 5′-CAAAAGCCCAGATTTTGAGG-3′/5′-TCTTTTACGGTGGTGA*CTGT-3′; pu.1*, 5′-ATGCTGCATCCGTACAGAATGG-3′/5′-GTGGTCGATAGATCTCTGTTTC-3′; and *ef1a*, 5′-CTTCTCAGGCTGACTGTGC-3′/5′-CCGCTAGCATTACCCTCC-3′.

Microscopy and Imaging

After WISH, the stained fish was mounted in 70% glycerol. Thereafter, whole mount or magnified bright field image was taken using a SPOT Flex camera mounted on Nikon AZ100 microscope (5×) or Nikon 80i microscope (20×/0.75 NA), respectively. Fluorescent image was captured with Carl Zeiss LSM510 confocal microscopy (40×/0.75 NA oil objective). All the images were processed using Adobe Photoshop 6.0.

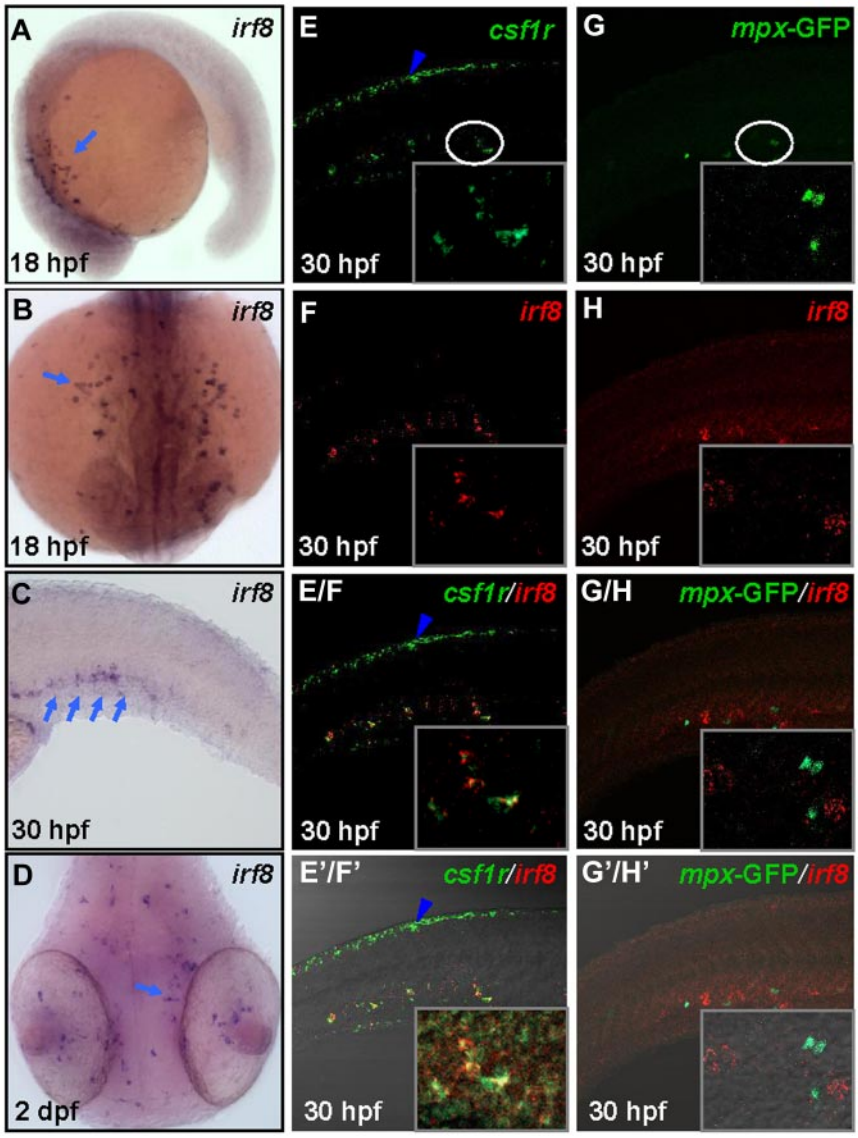

Figure 1. Expression pattern of *irf8* and costaining of *irf8* with *csf1r* and *mpx*. (A-B) WISH indicates *irf8* RNA expression in the yolk sac of 18 hpf WT embryos (n = 35/35). (C) WISH shows *irf8* RNA expression in the CHT[25,26] of 30 hpf WT embryo (n = 36/38). (D) WISH reveals *irf8* RNA expression in the head region of 2 dpf WT embryo (n = 33/39). (A-D) Blue arrows indicate the *irf8* signals. (E-F) Double WISH staining of *csf1r* and *irf8* RNA in the CHT of 30 hpf WT embryos (n = 32/35). (E/F) Superimposed image of panels E and F. (E′/F′) Merged view of E/F with DIC image. (G-H) Double staining of *mpx*-GFP and *irf8* RNA in the CHT of 30 hpf Tg (*mpx*:eGFP) embryos (n = 29/31). (G/H) Superimposed image of panels G and H. (G′/H′) Merged view of panel G/H with DIC image. (E,E/F,E′/F′) Blue arrowheads represent neural crest-derived pigment cells positive for *csf1r*. (E-G′/H′) Insets are higher magnification (×40) views of the circled region in panels E and G.

Results

Temporal-spatial expression of *irf8* during early zebrafish development

To investigate the role of Irf8 during zebrafish myelopoiesis, *irf8* was isolated by RT-PCR based on the sequence provided by the ZFIN database.[24] Protein sequence comparison revealed that zebrafish Irf8 shared 55% identity to the mammalian counterpart and contained a highly conserved DNA-binding domain at the N-terminus and an IRF association domain at the C-terminus (supplemental Figure 1, available on the *Blood* Web site; see the Supplemental Materials link at the top of the online article). To map the temporal and spatial expression patterns of *irf8* during zebrafish development, WISH was carried out with embryos at various developmental stages. As shown in Figure 1, *irf8* transcript was first detected at approximately 16 to 18 hpf in the rostral blood island (Figure 1A-B arrows, n = 35/35), where primitive myelopoiesis is known to initiate.[27-28] As embryos developed, *irf8*-expressing cells dispersed onto the yolk sac (data not shown) and by 30 hpf *irf8* was also emerged in the ventral tail region (Figure 1C arrows, n = 36/38), which is composed of in situ generated myeloid cells and rostral blood island-derived myeloid cells.[19,21] By 2 days post-fertilization (dpf), *irf8*$^+$ cells were found in the eyes and the brain (Figure 1D arrow, n = 33/39) in a manner recapitulating the distribution of microglia, a specialized macrophage in the central nervous system.[29] The WISH data suggest that *irf8* is expressed predominantly in myeloid cells during early zebrafish development. It is known that zebrafish primitive myelopoiesis gives rise to both macrophages[27] (microglia and circulating macrophages) and neutrophils,[21,30] which can be distinguished by the expression of macrophage marker *csf1r*[31] and neutrophilic marker *mpx*,[30] respectively. To address which sublineage of primitive myeloid cells expressed *irf8*, we performed double WISH, and result showed that *irf8* was expressed in the *csf1r*$^+$ myeloid cells, but not in the neural crest-derived pigment cells positive for *csf1r*[32] (Figure 1E-E′/F′, n = 32/35) and the myeloid cells expressing neutrophilic marker *mpx* (Figure 1G-G′/H′, n = 29/31). These data demonstrate that *irf8* expression is restricted to macrophage lineage during zebrafish primitive myelopoiesis.

Knockdown of Irf8 expression blocks macrophage development

The exclusive association of *irf8* expression with macrophages suggests that Irf8 may play an important role in macrophage development. To test this hypothesis, 2 MOs, *irf8*-MO^{sp} and *irf8*-MO^{atg}, which target *irf8* RNA splicing and *irf8* translation initiation, respectively, were designed to knock down *irf8* expression in zebrafish embryos. Sequencing of RT-PCR product and reporter assay confirmed that administration of *irf8*-MO^{sp} and *irf8*-MO^{atg} effectively blocked normal *irf8* RNA splicing and protein translation, respectively (supplemental Figure 2; supplemental Figure 3A, n = 38/40; supplemental Figure 3B, n = 36/36). As expected, identical phenotypes were observed in the embryos injected with *irf8*-MO^{sp} or *irf8*-MO^{atg} (Figures 2-3; supplemental Figure 3C-H). For the purpose of simplicity, *irf8*-MO^{sp} data were presented in most parts of this study.

To explore the effect of Irf8 knockdown on macrophages development, we first examined the expression of macrophage-specific marker *csf1r* in *irf8*-MO^{sp} injected embryos (*irf8*-MO^{sp} morphants) by WISH. Consistent with previous reports,[31,32] *csf1r* expression was readily detected in blood-born macrophage cells (Figure 2A blue arrow, n = 42/42) and neural crest-derived pigment cells (Figure 2A black arrowhead) in control embryos at 22 hpf. However, in *irf8*-MO^{sp} morphants, *csf1r* expression in macrophages (Figure 2B, n = 40/40; 2D, n = 36/36; Table 1), but not in the neural crest-derived pigment cells (Figure 2B,D black arrowheads), was absent. The suppression of *csf1r* expression in macrophages by *irf8*-MO^{sp} was specific because it could be restored by coinjection of in vitro transcribed WT *irf8* RNA (data not shown) or by heat shock induced Irf8 expression (supplemental Figure 2B-B′, n = 41/41; supplemental Figure 2C-C′, n = 25/33). Similar to that of *csf1r*, *apoeb* expression in microglia[29] was also deprived in 3 dpf *irf8*-MO^{sp} morphants (Figure 2E, n = 45/45; Figure 2F, n = 43/43; Table 1). These data strongly suggest that macrophage development is severely impaired in *irf8*-MO^{sp} morphants. To further support this notion, we took advantage of a bacterial phagocytosis assay, in which DsRed-labeled *E coli* were injected into the circulation of 40 hpf Tg(*mpx*:eGFP) embryos and functional macrophages were scored as phagocytes with large phagocytic foci at 30 minutes after injection.[23] Result showed that, whereas mature macrophages loaded with DsRed-labeled bacterial were readily seen in control embryos (Figure 2G blue arrows, n = 23/27), these large phagocytic cells were absent in *irf8*-MO^{sp} morphants (Figure 2H, n = 21/22). From these observations, we conclude that Irf8 is essential for macrophage development during primitive myelopoiesis.

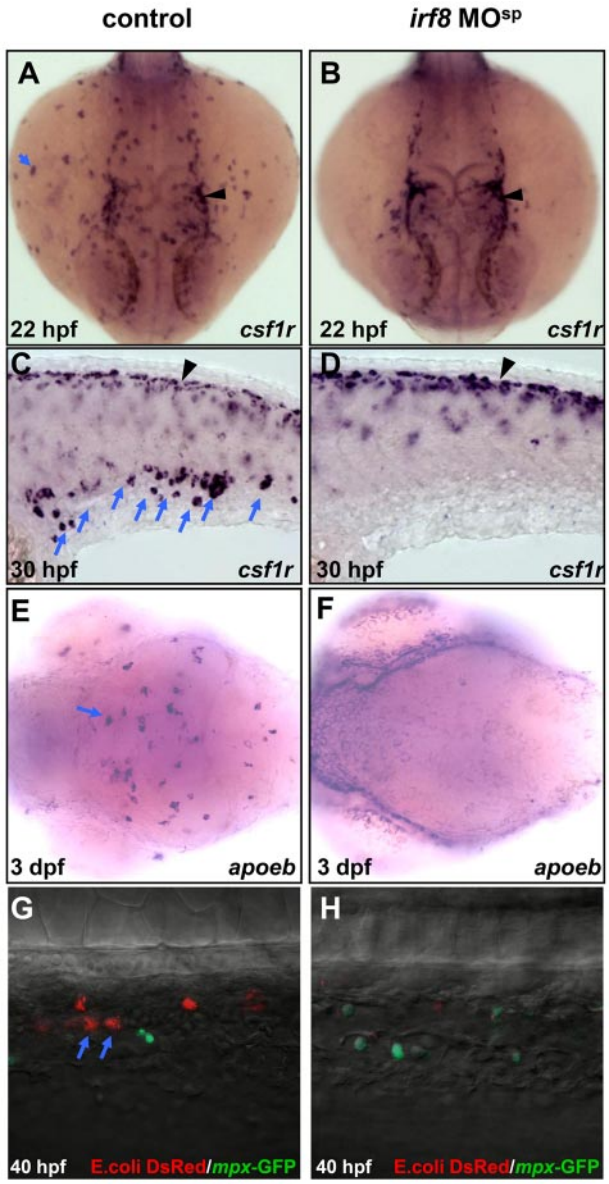

Figure 2. Depletion of macrophage population in *irf8* MO^{sp} morphants. (A-B) WISH shows *csf1r* RNA expression in the yolk sac of 22 hpf control embryo (n = 42/42) and 22 hpf *irf8* MO^{sp} morphant (n = 40/40). (C-D) WISH shows *csf1r* RNA expression in the CHT of 30 hpf control embryo (n = 38/38) and 30 hpf *irf8* MO^{sp} morphant (n = 36/36). Blue arrows indicate myeloid cells whereas black arrowheads represent neural crest-derived pigment cells. (E-F) WISH shows *apoeb* RNA expression in the brain region of 3 dpf control (n = 45/45) and *irf8* MO^{sp} morphant (n = 43/43) embryos. (G-H) Double staining of DsRed and GFP with antibodies shows macrophages loaded with *E. coli.* (red, blue arrows) and neutrophils (green) in the CHT of 40 hpf control embryo (n = 23/27) and *irf8* MO^{sp} morphant (n = 21/22).

Suppression of Irf8 function causes an expansion of neutrophil population

Previous studies in mice have documented that IRF8 mutant animals developed chronic myeloid leukemia with a profound increase of neutrophil number.[9,10] This prompted us to investigate whether suppression of Irf8 function in zebrafish also affected neutrophil development. WISH revealed a significant increase of neutrophilic marker *mpx, cebp1*, and *lyz* in *irf8*-MO^{sp} morphants compared with that in control embryos (Figure 3A-A′, n = 44/44; Figure 3B-B′, n = 47/48; Figure 3C-C′, n = 39/39; Figure 3D-D′, n = 38/38; supplemental Figure 4A-H′; Table 1) from 19 hpf. By 36 hpf, the number of cells positive for SB, a dye known to stain mature neutrophils,[21] was also increased in *irf8*-MO^{sp} morphants (Figure 3E, n = 53/53; Figure 3H, n = 49/49; Table 1), suggesting an expansion of neutrophil population in Irf8 knockdown embryos. To confirm that the expanded cells positive for *mpx, cebp1*, *lyz*, and SB were indeed neutrophils, video-enhanced DIC microscopic analysis was used to monitor macrophages and neutrophils in live 42 hpf Tg(*mpx*:eGFP) fish injected with or without *irf8*-MO^{sp}. In control embryos, mature neutrophils identified by their notable feature-active granules and mature macrophages, which contained large lysosomes loaded with the ingested debris but lacked granules, were seen[21] (Figure 3F-G, n = 11/11). However, in *irf8*-MO^{sp} morphants, a large number of neutrophils with motile granules emerged, and no typical macrophages were found (Figure

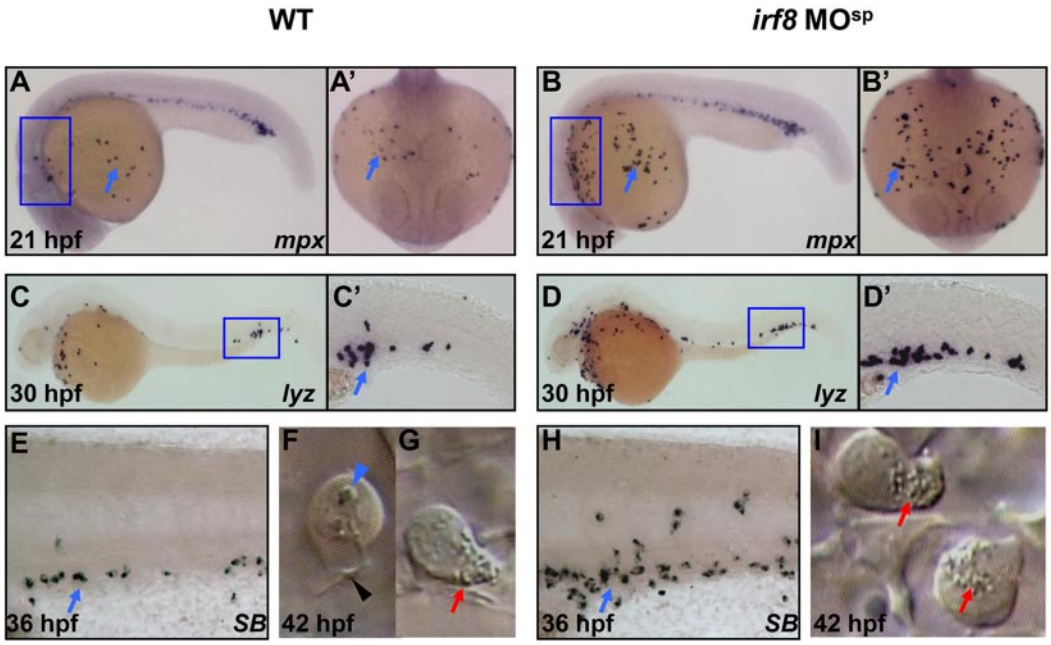

Figure 3. Expansion of neutrophils in *irf8* MO^{sp} morphants. (A-B′) WISH shows *mpx* RNA expression in 21 hpf control embryos (n = 44/44) and *irf8* MO^{sp} morphants (n = 47/48). (C-D′) WISH shows *lyz* RNA expression in 30 hpf control embryos (n = 39/39) and *irf8* MO^{sp} morphants (n = 38/38). (A-D′) Blue arrows indicate the WISH signals. (E,H) SB staining indicates mature neutrophils in the CHT region of 36 hpf control embryo (n = 53/53) and *irf8* MO^{sp} morphant (n = 49/49). (E,H) Blue arrows indicate the SB signals. (F-G,I) Video-enhanced DIC microscopy shows in vivo image of macrophages and neutrophils in 42 hpf control embryos (n = 11/11) and *irf8* MO^{sp} morphant (n = 10/10). (A′-B′) Dorsal views of the anterior yolk of the boxed regions in panels A and B (blue). (C′-D′) Higher magnification (×20) views of the boxed regions (blue) in panels C and D. (F) Blue and black arrowheads indicate the lysosome inside the macrophage and the long filopodia of macrophage, respectively. (G,I) Red arrows represent granules in neutrophils.

3I, n = 10/10). These data demonstrate that suppression of Irf8 function causes an expansion of neutrophil population.

The expanded neutrophils in *irf8* morphants derive from the *lcp1*$^+$ myeloid progenitors or macrophages

Three possible mechanisms could lead to the expansion of neutrophils in *irf8* morphants: (1) prolonged survival of *irf8*-deficient neutrophils, (2) accelerated neutrophil proliferation, and (3) aberrant macrophage versus neutrophil fate decision. To distinguish these mechanisms, we first examined whether *irf8*-deficient neutrophils had a suppressed apoptotic program by identifying apoptotic cells with acridine orange staining. Comparable acridine orange$^+$ apoptotic cells were observed between *irf8*-MO^{sp} morphants and controls (data not shown), suggesting that the expanded neutrophils in *irf8*-MO^{sp} morphants do not result from prolonged survival of these cells. To probe the cell cycle status of neutrophils in *irf8*-MO^{sp} morphants, we used the BrdU incorporation assay to monitor the cycling cells in S phase. Tg(*mpx*:eGFP) control or *irf8*-MO^{sp}-injected embryos were pulse labeled with BrdU and immediately fixed for anti-BrdU and anti-GFP staining.[20] In control embryos, approximately 20% of *mpx*-GFP-positive (*mpx*-GFP$^+$) neutrophils were BrdU-positive (BrdU$^+$) (representing cells in S phase), whereas in *irf8*-MO^{sp} morphants, the percentage of BrdU$^+$*mpx*-GFP$^+$ neutrophils rose to 28% (Figure 4A, n = 8/8; Figure 4B, n = 7/7; Figure 4E). This result seemed to suggest an accelerated neutrophil proliferation in *irf8*-MO^{sp} morphants. However, when mitotic neutrophil number was estimated by antiphosphohistone H3 (pH3) antibody staining,[33] the percentage of pH3$^+$ *mpx*-GFP$^+$ neutrophils in the M phase was unexpectedly decreased in *irf8*-MO^{sp} morphants compared with that in control embryos (Figure 4C, n = 8/8; Figure 4D, n = 7/7; Figure 4E). The opposing alteration in S and M phase profile exhibited by *mpx*-GFP$^+$ neutrophils in *irf8*-MO^{sp} morphants suggests that Irf8-deficient neutrophils possess unusual but not accelerated proliferative cycles. Thus, the increased neutrophil population in *irf8*-MO^{sp} morphants could not be accounted by accelerated neutrophil proliferation, which necessitates a concurrently elevated S and M phase profile. Hence, the only logic interpretation for neutrophil expansion in *irf8*-MO^{sp} morphants is fate transition from myeloid progenitors or macrophages. This interpretation predicts that there will be no overt difference in cell number and cell cycle profile of entire myeloid population between *irf8*-MO^{sp} morphants and controls. As anticipated, the overall number of cells positive for *lcp1*, a pan-myeloid marker identifying all myeloid subsets, including *csf1r*$^+$ macrophages and *mpx*$^+$ neutrophils,[31] was comparable between *irf8*-MO^{sp} morphants and control embryos (Figure 4N, n = 35/35; Figure 4O, n = 29/29; Figure 4P; supplemental Figure

Table 1. Quantification of myeloid cells in control and *irf8* MO^{sp} embryos

	Genotype	
Stage/marker	**Control (mean ± SE)**	***irf8* MO^{sp} (mean ± SE)**
22 hpf		
csf1r	51.58 ± 4.44 (n = 12)	0* (n = 11)
mpx	19.20 ± 1.10 (n = 15)	66.86 ± 4.15* (n = 14)
30 hpf		
csf1r	111.62 ± 5.40 (n = 13)	0* (n = 17)
lyz	77.00 ± 3.41 (n = 15)	207.56 ± 6.70* (n = 16)
36 hpf		
SB	93.07 ± 4.32 (n = 14)	282.50 ± 9.08* (n = 14)
3 dpf		
apoeb	20.83 ± 1.97 (n = 18)	0* (n = 20)

Values in parentheses indicate the number of embryos quantified.
*Significant statistical difference with corresponding control (*t* test, $P < .01$).

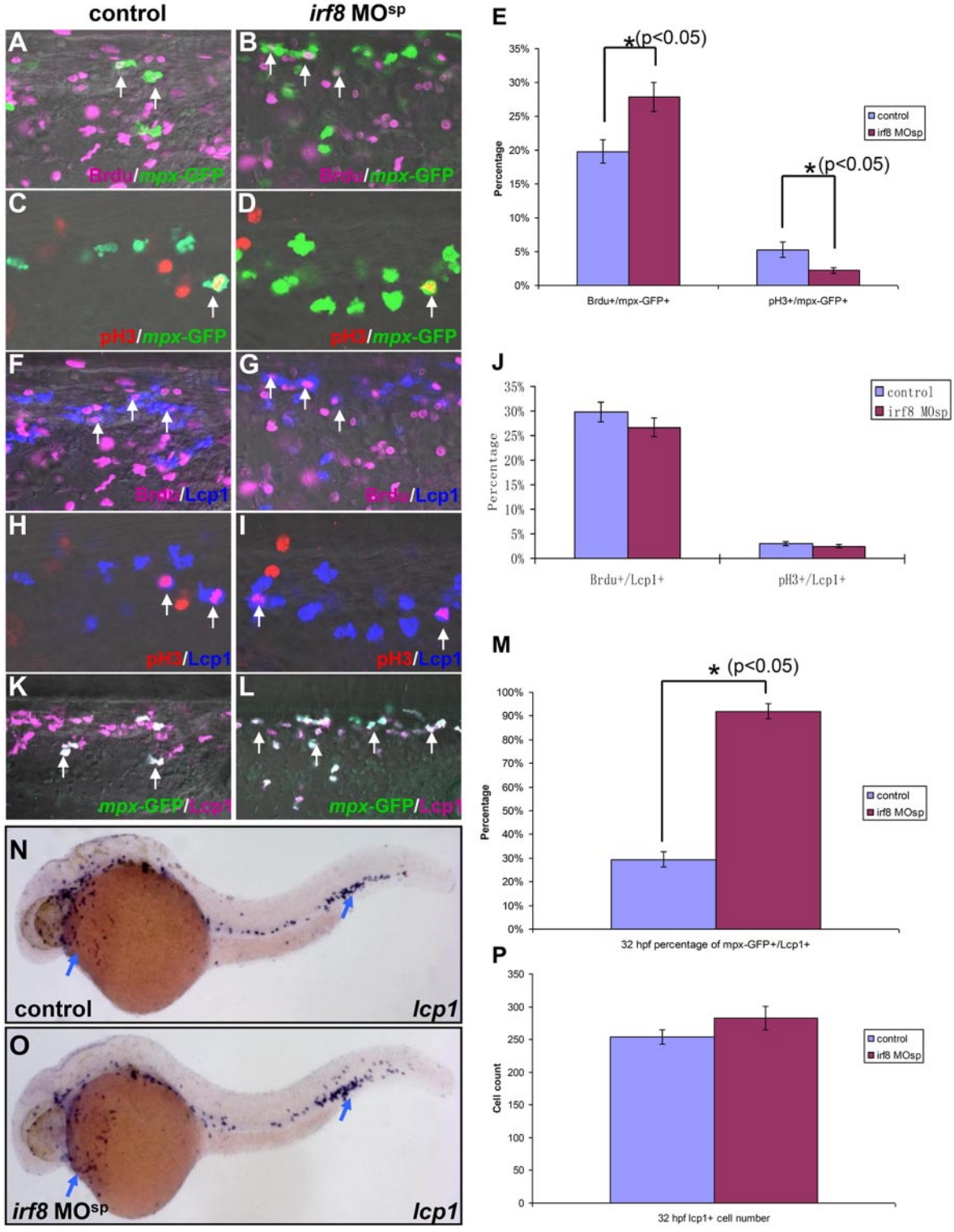

Figure 4. Cell cycle profile of primitive myeloid cells in *irf8* MO^{sp} morphants. (A-B) BrdU and GFP double staining indicates the neutrophils in S phase in the CHT region of 32 hpf Tg(*mpx*:eGFP) control embryo (n = 8/8) and *irf8* MO^{sp} morphant (n = 7/7). (C-D) pH3 and GFP double staining reveals the neutrophils in M phase in the CHT region of 32 hpf Tg(*mpx*:eGFP) control embryo (n = 8/8) and *irf8* MO^{sp} morphant (n = 7/7). (E) Histogram represents the percentage of BrdU$^+$*mpx*-GFP$^+$ (S phase) and pH3$^+$*mpx*-GFP$^+$ (M phase) cells in 32 hpf Tg(*mpx*:eGFP) control embryos and *irf8* MO^{sp} morphants (n ≥ 7, mean ± SE). *Statistical differences with corresponding control (*t* test, $P < .05$). (F-G) BrdU and Lcp1 double staining shows the overall myeloid cells in S phase in the CHT of 32 hpf Tg(*mpx*:eGFP) control embryo (n = 8/8) and *irf8* MO^{sp} morphant (n = 7/7). (H-I) pH3 and Lcp1 double staining shows the overall myeloid cells in M phase in the CHT of 32 hpf Tg(*mpx*:eGFP) control embryo (n = 8/8) and *irf8* MO^{sp} morphant (n = 7/7). (J) Histogram reveals the percentage of BrdU$^+$Lcp1$^+$ (S phase) and pH3$^+$/Lcp1$^+$ (M phase) cells in 32 hpf Tg(*mpx*:eGFP) control embryos and *irf8* MO^{sp} morphants (n ≥ 7, mean ± SE). (K-L) GFP and Lcp1 double staining presents neutrophils in the CHT of 32 hpf Tg(*mpx*:eGFP) control embryo (n = 8/8) and *irf8* MO^{sp} morphant (n = 7/7). (M) Histogram shows the percentage of *mpx*-GFP$^+$Lcp1$^+$ cells (neutrophils) in 32 hpf Tg(*mpx*:eGFP) control embryos and *irf8* MO^{sp} morphants (n ≥ 7, mean ± SE). *Statistical differences with corresponding control (*t* test, $P < .05$). White arrows indicate the costaining of BrdU and GFP in panels A and B, pH3 and GFP in panels C and D, BrdU and Lcp1 in panels F and G, pH3 and Lcp1 in panels H and I, and GFP and Lcp1 in panels K and L. (N-O) WISH indicates *lcp1* RNA expression in 32 hpf control embryo (n = 35/35) and *irf8* MO^{sp} morphant (n = 29/29). Blue arrows represent the WISH signals. (P) Histogram reveals the overall myeloid cell number positive for *lcp1* in 32 hpf control embryos and *irf8* MO^{sp} morphants (n ≥ 10, mean ± SE).

5F-H). Consistent with the fate switching hypothesis, *mpx*$^+$*lcp1*$^+$ double-positive cells accounted for approximately 30% of total *lcp1*$^+$ cells at both early and late stage in control embryos, whereas in *irf8*-MO^{sp} morphants almost all the *lcp1*$^+$ cells were *mpx*$^+$ (Figure 4K, n = 8/8; Figure 4L, n = 7/7; Figure 4M; supplemental Figure 5A-E). More importantly, *lcp1*$^+$ myeloid population in *irf8*-MO^{sp} morphants had a cell cycle profile identical to *lcp1*$^+$ myeloid population in controls (Figure 4F,H, n = 8/8; Figure 4G,I, n = 7/7; Figure 4J). It thus suggests that the paradoxical cell cycle profile of Irf8-deficient neutrophils probably reflects a composite profile of normal neutrophils and those arising from fate transition, thus adapting cell cycle feature of myeloid progenitors or macrophages. Collectively, our data support the notion that the expansion of neutrophil population when Irf8 is deficient results from a fate switching from *lcp1*$^+$ myeloid progenitors or macrophages.

Overexpression of Irf8 promotes the development of macrophages but suppresses that of neutrophils

To further support the conclusion that Irf8 indeed functions as a critical determinant for macrophage versus neutrophil fate, we created a stable transgenic line Tg(*hsp70*:Irf8^{myc}) in which a Myc-tagged *irf8* (*irf8*^{myc}) cDNA was placed under the control of a heat shock protein (*hsp*) 70 promoter.[22] We reasoned that overexpression of Irf8^{myc} in WT embryos would produce a myeloid phenotype opposite to that of *irf8*-MO^{sp} morphants. When raised at 28.5°C, Tg(*hsp70*:Irf8^{myc}) fish did not produce detectable exogenous Irf8^{myc} and displayed a normal primitive myelopoiesis (Figure 5A, n = 32/32; Figure 5C-C′, n = 22/22; Figure 5D-D′, n = 18/18; Figure 5H-H′, n = 17/17; Figure 5I-I′, n = 20/20; Figure 5G,L). Heat shock treatment of Tg(*hsp70*:Irf8^{myc}) embryos (at 11 hpf, 39.5°C for 1.5 hours) induced a high level of Irf8^{myc} expression (Figure 5B, n = 25/30). As a result, at 26 hpf, these heat shock-treated Tg(*hsp70*:Irf8^{myc}) embryos displayed an approximately 50% increase (Figure 5G, n ≥ 9) in *csf1r*$^+$ macrophage number (Figure 5C-G) and an approximately 40% decrease (Figure 5L, n ≥ 10) in *mpx*$^+$ neutrophil number (Figure 5H-L) compared with untreated embryos. These data demonstrate that overexpression of Irf8 promotes the formation of macrophages at the expense of neutrophil development. This further strengthens the notion that Irf8 is an essential determinant for macrophage versus neutrophil fate during primitive myelopoiesis.

Irf8 acts downstream of Pu.1 during primitive myelopoiesis

It is well known that Ets transcription factor PU.1/Spi-1 is a master regulator involved in the earliest step of myeloid cell development in mice.[34] Similarly, suppression of Pu.1 function by MO in zebrafish embryos blocks the development of both macrophages and neutrophils.[35,36] Based on these studies, we speculated that Irf8 was probably a downstream factor of Pu.1. To confirm this speculation, genetic epistasis analysis was performed. WISH revealed that *irf8* transcript was drastically reduced in *pu.1* morphants (Figure 6A, n = 35/35; Figure 6B, n = 28/29), whereas *pu.1* expression was not affected by *irf8* knockdown (Figure 6C, n = 31/31; Figure 6D, n = 27/27; Figure 6E, n = 30). These observations indicate that Irf8 acts downstream of Pu.1 during primitive myelopoiesis. We therefore next asked whether forced expression of Irf8 in *pu.1* morphants was able to rescue the macrophage defect. To test that, Tg(*hsp70*:Irf8^{myc}) embryos were injected with *pu.1* MO, exposed to heat shock treatment, and then examined for indications of macrophage marker *csf1r*, microglia marker *apoeb*, and bacterial-phagocytosis activity. To our surprise, although heat shock treatment induced a high level of Irf8^{myc} expression (Figure 6G, n = 26/31), it failed to restore the macrophage development in the *pu.1* knockdown embryos as shown by the lack of *csf1r* (Figure 6H, n = 41/41; Figure 6I, n = 45/46; Figure 6J, n = 51/51) and *apoeb* (Figure 6K, n = 43/43; Figure 6L, n = 37/37; Figure 6M, n = 41/41) expression as well as bacteria-phagocytosis activity (Figure 6N, n = 27/30; Figure 6O, n = 25/29; Figure 6P, n = 30/32). These results demonstrate that Irf8 acts downstream of Pu.1 but is insufficient to promote macrophage formation when Pu.1 function is suppressed.

Discussion

In this report, we have cloned zebrafish *irf8* gene and characterized its expression and function in myeloid development. During zebrafish embryogenesis, the expression of zebrafish *irf8* is predominantly associated with primitive macrophages but not other blood lineages, including neutrophils, erythrocytes, and T lymphocytes (H.L., Z.L., unpublished data, January 2010). Similarly, in adult mice, *IRF8* was reported to be exclusively expressed in hematopoietic cells, including adult cells of monocyte/macrophage lineage, B lymphocytes, and activated T lymphocytes.[8] Thus, it appears that there is a conserved expression profile of *IRF8* at different phases of hematopoiesis among evolutionarily divergent species. This conserved expression pattern is reflected by similar disturbance of zebrafish embryonic hematopoiesis and murine adult hematopoiesis when Irf8 is inactivated. Irf8-deficient zebrafish embryos contain an expanded neutrophilic compartment but fail in the establishment of macrophage population. On the other hand, erythrocytes and T cells appear to be unaffected in Irf8 knockdown embryos (unpublished data). This phenotype is, to a large extent, similar to that of IRF8 null and BHX mice, which harbor a loss-of-function mutation in the *IRF8* gene.[9,10] Likewise, erythrocyte and T-cell development is grossly normal in IRF8-deficient mice.[9,10] Notably, B-cell development in these IRF8 mutant mice is compromised.[37] However, because of the late arising of B cells during zebrafish development and transient nature of MO knockdown, we are hindered from analyzing Irf8 depletion on B-cell ontogeny in zebrafish. Nevertheless, the overall similar functional requirement of Irf8 during zebrafish primitive/embryonic myelopoiesis and mice definitive/adult myelopoiesis underscores parallels in the transcriptional regulatory program among these 2 processes and the validity of extrapolating insights from studying zebrafish primitive myelopoiesis to myelopoiesis in higher organisms.

Our study shows that knockdown of Irf8 leads to a depletion of macrophages with a concomitant expansion of neutrophil population. This skewed myeloid lineage development is not accompanied by the concomitant increase of the number of total primitive myeloid population. Apoptotic assay and cell cycle analyses indicate that the expanded neutrophil population is not ascribed to accelerated proliferative cycle or prolonged cell survival. On the other hand, overexpression of Irf8 in zebrafish embryos is able to drive myeloid development toward macrophage lineage. Thus, our data favor the role of Irf8 in regulating macrophage versus neutrophil fate choice and oppose the model whereby IRF8 differentially regulates the survival, proliferation, and differentiation of individual lineage in adult mice.[38-40] This result is also consistent with an early in vitro study, which reported that reconstitution of immortal mouse IRF8-null cell lines by IRF8 directed macrophage differentiation of these cells, which otherwise adopted neutrophilic fates.[14] It remains unknown whether fate

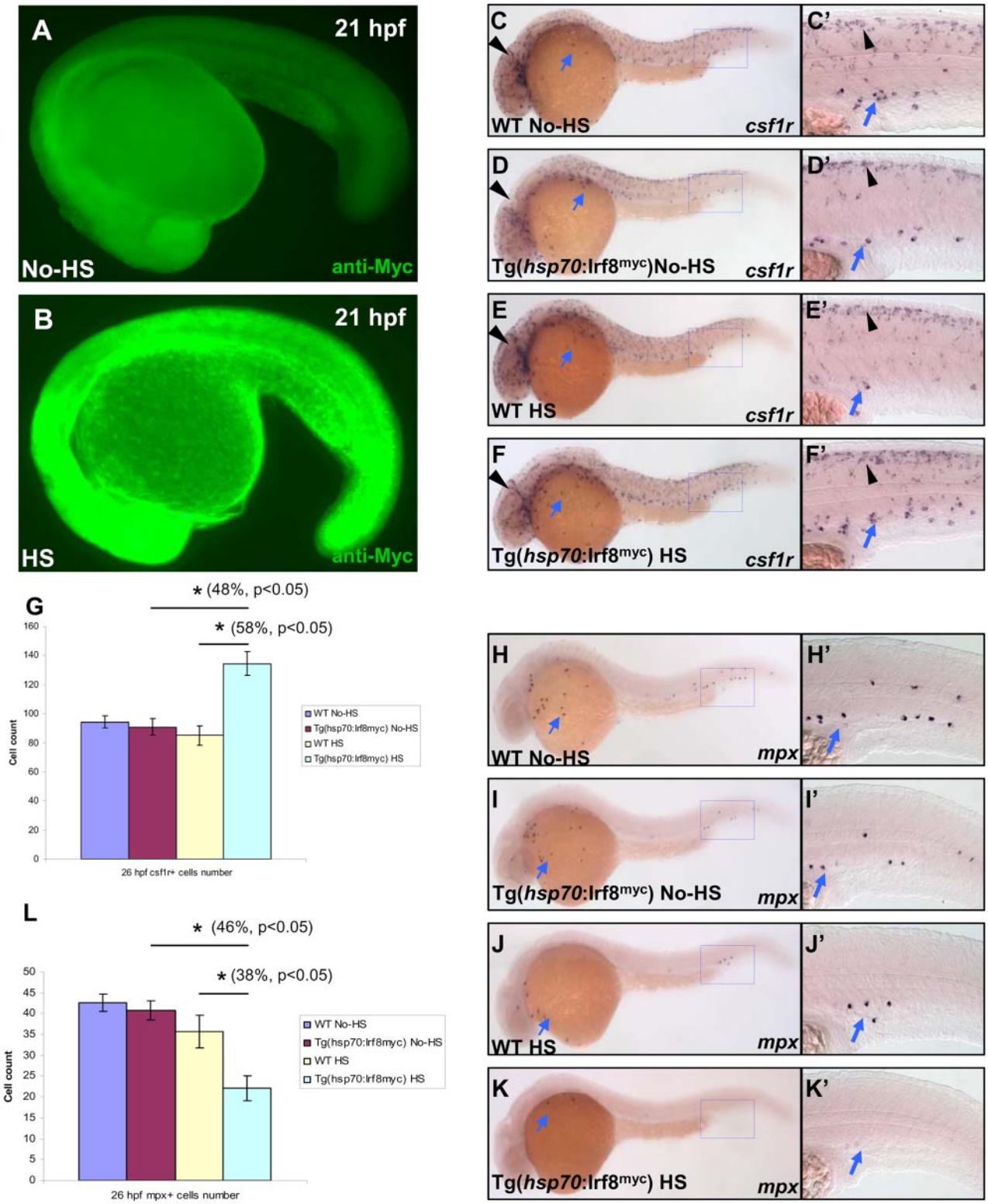

Figure 5. Overexpression of Irf8 promotes the development of macrophages but suppresses that of neutrophils. (A-B) Anti-Myc antibody staining indicates a significant induction of Irf8^{myc} protein expression in the heat shock-treated (HS) Tg(*hsp70*:Irf8^{myc}) embryo (n = 25/30) compared with the untreated (No-HS) embryo (n = 32/32). (C-F′) WISH shows *csf1r* RNA expression in 26 hpf untreated (No-HS) WT (n = 22/22) and Tg(*hsp70*:Irf8^{myc}) (n = 18/18) and heat shock-treated (HS) WT (n = 16/16) and Tg(*hsp70*:Irf8^{myc}) (n = 10/13) embryos. (C′-F′) Higher magnification (×20) views of the boxed regions (blue) in panels C, D, E, and F, respectively. (G) Histogram represents the overall number of *csf1r*$^{+}$ cells (macrophages) in panels C, D, E, and F (n ≥ 9, mean ± SE). *Statistical differences with corresponding control (48% increase compared with No-HS Tg(*hsp70*:Irf8^{myc}), *t* test, $P < .05$; 58% increment compared with HS WT *t* test, $P < .05$). (H-K′) WISH shows *mpx* RNA expression in 26 hpf untreated (No-HS) WT (n = 17/17) and Tg(*hsp70*:Irf8^{myc}) (n = 20/20) and heat shock-treated (HS) WT (n = 13/15) and Tg(*hsp70*:Irf8^{myc}) (n = 11/16) embryos. (H′-K′) Higher magnification (×20) views of the boxed regions (blue) in panels H, I, J, and K, respectively. (L) Histogram represents the overall number of *mpx*$^{+}$ cells (neutrophils) in panels H, I, J, and K (n ≥ 10, mean ± SE). *Statistical differences with corresponding control (46% decrease compared with No-HS Tg(*hsp70*:Irf8^{myc}), *t* test, $P < .05$; 38% reduction compared with HS WT, *t* test, $P < .05$). (C-F′,H-K′) Blue arrows indicate myeloid cells positive for *csf1r* and *mpx*, respectively. (C-F′) Black arrowheads indicate neural crest-derived pigment cells positive for *csf1r*.

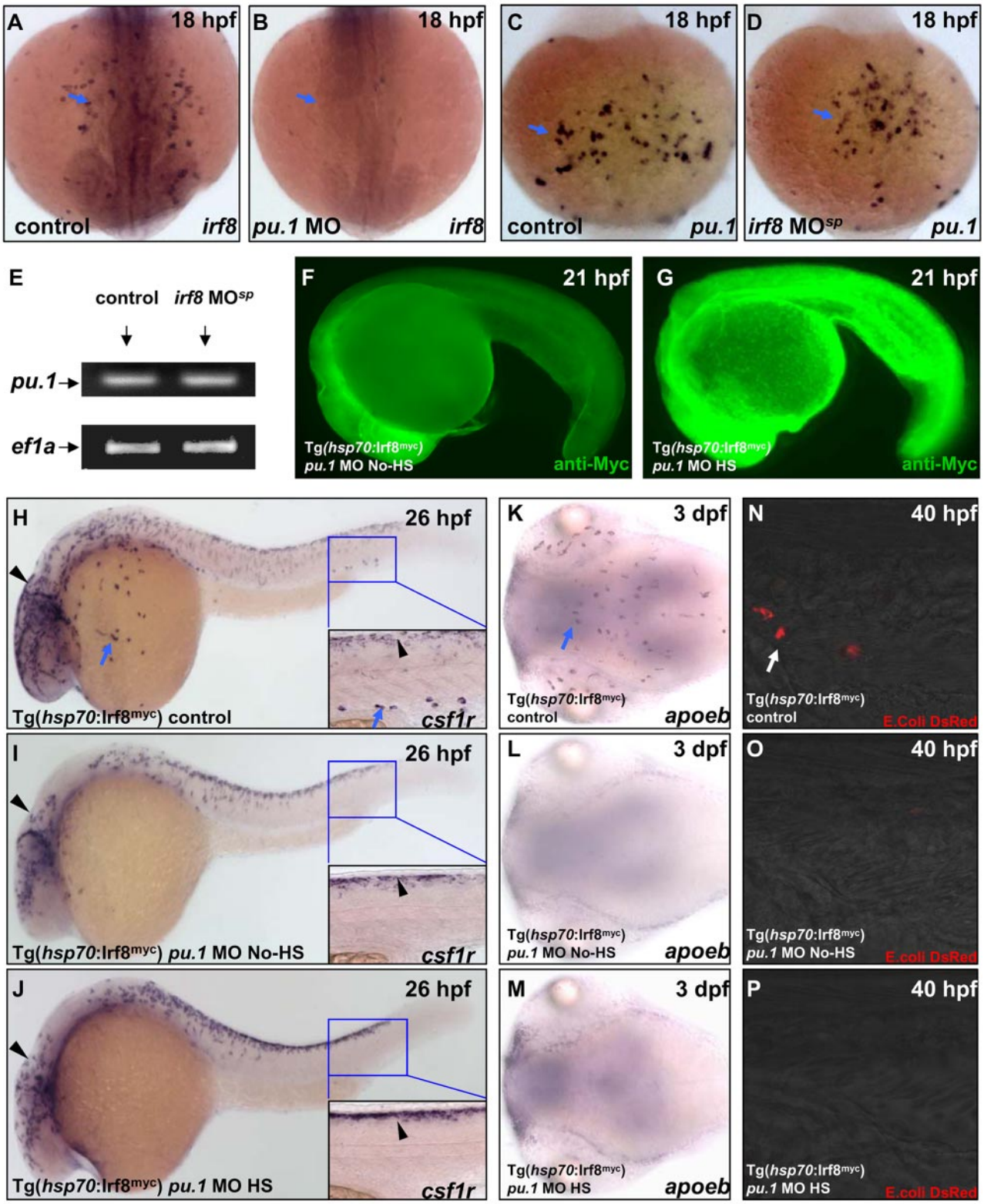

Figure 6. Irf8 is downstream of Pu.1. (A-B) WISH indicates *irf8* RNA expression in the yolk sac of 18 hpf control embryo (n = 35/35) and *pu.1* morphant (n = 28/29). (C-D) WISH shows *pu.1* RNA expression in the yolk sac of 18 hpf control embryo (n = 31/31) and *irf8* MO^{sp} morphant (n = 27/27). (E) RT-PCR analysis confirms a similar level of *pu.1* expression in 18 hpf control embryos (left lane) and *irf8* MO^{sp} morphants (right lane). (F-G) Anti-Myc staining reveals a significant induction of Irf8^{myc} protein expression in the heat shock-treated (HS) *pu.1* morphant (n = 26/31) compared with the untreated (No-HS) *pu.1* morphant (n = 33/33). (H-J) WISH indicates *csf1r* expression in 26 hpf untreated control embryo (n = 41/41), untreated (No-HS) *pu.1* morphant (n = 45/46), and heat shock-treated (HS) *pu.1* morphant (n = 51/51). (H-J) Insets are higher magnification (×20) views of the boxed region (blue). (K-M) WISH reveals *apoeb* RNA expression in the brain of 3 dpf untreated control embryo (n = 43/43), untreated (No-HS) *pu.1* morphant (n = 37/37), and heat shock-treated (HS) *pu.1* morphant (n = 41/41). (A-D,H,K) Blue arrows indicate *csf1r*$^{+}$ macrophages. (H-J) Black arrowheads represent neural crest-derived pigment cells positive for *csf1r*. (N-P) DsRed shows macrophages loaded with *E coli* (red, white arrows) in the CHT of 40 hpf untreated control embryo (n = 27/30), untreated (No-HS) *pu.1* morphant (n = 25/29), and heat shock-treated (HS) *pu.1* morphant (n = 30/32).

transition incurred by altered IRF8 expression occurs at the level of common myeloid progenitors or committed differentiating progeny. It will be of interest to determine the consequence of specifically modulating IRF8 level in individual myeloid lineage.

The molecular mechanism by which IRF8 executes its lineage selection role is still obscure. Previous studies revealed that IRF8 in conjunction with IRF-1 and IRF-2 negatively regulated some interferon-inducible gene via binding to interferon-stimulated response element,[41-43] whereas IRF8, together with PU.1, stimulated the activity of promoters harboring Ets-IRF composite element.[42,44-48] It is conceivable to speculate that one mode of IRF8 action could be to suppress the expression of a cohort of neutrophil-specific genes and, at the same time, activate a group of macrophage-specific genes via interaction with different partners. This postulation correlates with the findings that macrophage formation requires high PU.1 activity in mammalian culture cells[49] and zebrafish (H.L., Z.L., unpublished data, January 2010), and forced expression of Irf8 alone in *pu.1* knockdown embryos is insufficient to restore macrophage development (Figure 6H-P). In myeloid versus erythroid fate choice, Pu.1 and Gata1 have been shown to antagonize each other to promote myeloid and erythroid fates, respectively.[35,36] Thus, an alternative mode of Irf8 action could be to modulate a set of neutrophil- and macrophage-specific genes through antagonizing an anonymous key neutrophilic fate-promoting factor. These 2 modes of Irf8 action are not mutually exclusive. It is probable that the myeloid lineage output regulated by Irf8 is the consequence of the coordinated efforts of these 2 modes.

Acknowledgments

The authors thank Drs S. A. Renshaw (University of Sheffield, United Kingdom) and P. W. Ingham (University of Sheffield, United Kingdom; Institute of Molecular and Cell Biology, Singapore) for providing Tg(*mpx*:eGFP) fish, and Dr P. Herbomel (Institute Pasteur, France) for his instrumental help in setting up the video-enhanced DIC system.

This work was supported by the Area of Excellence Scheme established under the University Grants Committee of the Hong Kong Special Administrative Region (grant AoE/B-15/01) and the Research Grants Council of the Hong Kong Special Administrative Region (General Research Fund grants 662808 and 663109).

Authorship

Contribution: L.L., H.J., J.X., and Y.S. performed experiments; L.L., H.J., J.X., and Z.W. designed the research and analyzed data; and L.L., H.J., and Z.W. participated in the preparation of manuscript.

Conflict-of-interest disclosure: The authors declare no competing financial interests.

Correspondence: Zilong Wen, State Key Laboratory of Molecular Neuroscience, Department of Biochemistry, Hong Kong University of Science and Technology, Clear Water Bay, Kowloon, Hong Kong, People's Republic of China; e-mail: zilong@ust.hk.

References

1. Heissig B, Nishida C, Tashiro Y, et al. Role of neutrophil-derived matrix metalloproteinase-9 in tissue regeneration. *Histol Histopathol.* 2010;25(6):765-770.
2. Lin SL, Li B, Rao S, et al. Macrophage Wnt7b is critical for kidney repair and regeneration. *Proc Natl Acad Sci U S A.* 2010;107(9):4194-4199.
3. Mukhopadhyay S, Pluddemann A, Gordon S. Macrophage pattern recognition receptors in immunity, homeostasis and self tolerance. *Adv Exp Med Biol.* 2009;653:1-14.
4. Rosenbauer F, Tenen DG. Transcription factors in myeloid development: balancing differentiation with transformation. *Nat Rev Immunol.* 2007;7(2):105-117.
5. Metcalf D. The molecular control of cell division, differentiation commitment and maturation in haemopoietic cells. *Nature.* 1989;339(6219):27-30.
6. Driggers PH, Ennist DL, Gleason SL, et al. An interferon gamma-regulated protein that binds the interferon-inducible enhancer element of major histocompatibility complex class I genes. *Proc Natl Acad Sci U S A.* 1990;87(10):3743-3747.
7. Sharf R, Azriel A, Lejbkowicz F, et al. Functional domain analysis of interferon consensus sequence binding protein (ICSBP) and its association with interferon regulatory factors. *J Biol Chem.* 1995;270(22):13063-13069.
8. Paun A, Pitha PM. The IRF family, revisited. *Biochimie.* 2007;89(6):744-753.
9. Holtschke T, Löhler J, Kanno Y, et al. Immunodeficiency and chronic myelogenous leukemia-like syndrome in mice with a targeted mutation of the ICSBP gene. *Cell.* 1996;87(2):307-317.
10. Turcotte K, Gauthier S, Tuite A, Mullick A, Malo D, Gros P. A mutation in the Icsbp1 gene causes susceptibility to infection and a chronic myeloid leukemia-like syndrome in BXH-2 mice. *J Exp Med.* 2005;201(16):881-890.
11. Aliberti J, Tamura T, Gongora C, et al. Essential role for ICSBP in the in vivo development of murine CD8alpha+ dendritic cells. *Blood.* 2003;101(3):305-310.
12. Tailor P, Tamura T, Morse HC III, Ozato K. The BXH2 mutation in IRF8 differentially impairs dendritic cell subset development in the mouse. *Blood.* 2008;111(4):1942-1945.
13. Zhao B, Takami M, Yamada A, et al. Interferon regulatory factor-8 regulates bone metabolism by suppressing osteoclastogenesis. *Nat Med.* 2009;15(9):1066-1071.
14. Tamura T, Nagamura-Inoue T, Shmeltzer Z, Kuwata T, Ozato K. ICSBP directs bipotential myeloid progenitor cells to differentiate into mature macrophages. *Immunity.* 2000;13(2)155-165.
15. Moore MA, Metcalf D. Ontogeny of the haemopoietic system: yolk sac origin of in vivo and in vitro colony forming cells in the developing mouse embryo. *Br J Haematol.* 1970;18(3):279-296.
16. Orkin SH, Zon LI. Hematopoiesis: an evolving paradigm for stem cell biology. *Cell.* 2008;132(4):631-644.
17. Renshaw SA, Loynes CA, Trushell DM, Elworthy S, Ingham PW, Whyte MKA. Transgenic zebrafish model of neutrophilic inflammation. *Blood.* 2006;108(13):3976-3978.
18. Westerfield M. *The Zebrafish Book*: *A Guide for the Laboratory Use of zebrafish* (*Danio rerio*). 3rd ed. Eugene, OR: University of Oregon Press; 1995.
19. Jin H, Sood R, Xu J, et al. Definitive hematopoietic stem/progenitor cells manifest distinct differentiation output in the zebrafish VDA and PBI. *Development.* 2009;136(4):647-654.
20. Wallace KN, Akhter S, Smith EM, Lorent K, Pack M. Intestinal growth and differentiation in zebrafish. *Mech Dev.* 2005;122(2):157-173.
21. Le Guyader D, Redd MJ, Colucci-Guyon E, et al. Origins and unconventional behavior of neutrophils in developing zebrafish. *Blood.* 2008;111(1):132-141.
22. Halloran MC, Sato-Maeda M, Warren JT, et al. Laser-induced gene expression in specific cells of transgenic zebrafish. *Development.* 2000;127(9):1953-1960.
23. van der Sar AM, Musters RJ, van Eeden FJ, et al. Zebrafish embryos as a model host for the real time analysis of Salmonella typhimurium infections. *Cell Microbiol.* 2003;5(9):601-611.
24. Stein C, Caccamo M, Laird G, Leptin M. Conservation and divergence of gene families encoding components of innate immune response systems in zebrafish. *Genome Biol.* 2007;8(11):R251.
25. Jin H, Xu J, Wen ZL. Migratory path of definitive hematopoietic stem/progenitor cells during zebrafish development. *Blood.* 2007;109(12):5208-5214.
26. Murayama E, Kissa K, Zapata A, et al. Tracing hematopoietic precursor migration to successive hematopoietic organs during zebrafish development. *Immunity.* 2006;25(6):963-975.
27. Herbomel P, Thisse B, Thisse C. Ontogeny and behaviour of early macrophages in the zebrafish embryo. *Development.* 1999;126(17):3735-3745.
28. Lieschke GJ, Oates AC, Paw BH, et al. Zebrafish SPI-1 (PU.1) marks a site of myeloid development independent of primitive erythropoiesis: implications for axial patterning. *Dev Biol.* 2002;246(2):274-295.
29. Peri F, Nusslein-Volhard C. Live imaging of neuronal degradation by microglia reveals a role for v0-ATPase a1 in phagosomal fusion in vivo. *Cell.* 2008;133(5):916-927.
30. Lieschke GJ, Oates AC, Crowhurst MO, Ward AC, Layton JE. Morphologic and functional characterization of granulocytes and macrophages in embryonic and adult zebrafish. *Blood.* 2001;98(10):3087-3096.
31. Meijer AH, van der Sar AM, Cunha C, et al. Identification and real-time imaging of a myc-expressing neutrophil population involved in inflammation

and mycobacterial granuloma formation in zebrafish. *Dev Comp Immunol.* 2008;32(1):36-49.

32. Parichy DM, Ransom DG, Paw B, Zon LI, Johnson SL. An orthologue of the kit-related gene fms is required for development of neural crest-derived xanthophores and a subpopulation of adult melanocytes in the zebrafish, Danio rerio. *Development.* 2000;127(14):3031-3044.
33. Hendzel MJ, Wei Y, Mancini MA, et al. Mitosis-specific phosphorylation of histone H3 initiates primarily within pericentromeric heterochromatin during G2 and spreads in an ordered fashion coincident with mitotic chromosome condensation. *Chromosoma.* 1997;106(6):348-360.
34. Scott EW, Simon MC, Anastasi J, Singh H. Requirement of transcription factor PU.1 in the development of multiple hematopoietic lineages. *Science.* 1994;265(5178):1573-1577.
35. Galloway JL, Wingert RA, Thisse C, Thisse B, Zon LI. Loss of gata1 but not gata2 converts erythropoiesis to myelopoiesis in zebrafish embryos. *Dev Cell.* 2005;8(1):109-116.
36. Rhodes J, Hagen A, Hsu K, et al. Interplay of PU.1 and gata1 determines myelo-erythroid progenitor cell fate in zebrafish. *Dev Cell.* 2005;8(1):97-108.
37. Wang H, Lee CH, Qi C, et al. IRF8 regulates B-cell lineage specification, commitment, and differentiation. *Blood.* 2008;112(10):4028-4038.
38. Gabriele L, Phung J, Fukumoto J, et al. Regulation of apoptosis in myeloid cells by interferon consensus sequence-binding protein. *J Exp Med.* 1999;190(3):411-421.
39. Schmidt M, Bies J, Tamura T, Ozato K, Wolff L. The interferon regulatory factor ICSBP/IRF-8 in combination with PU.1 up-regulates expression of tumor suppressor p15(Ink4b) in murine myeloid cells. *Blood.* 2004;103(11):4142-4149.
40. Tamura T, Kong HJ, Tunyaplin C, Tsujimura H, Calame K, Ozato K. ICSBP/IRF-8 inhibits mitogenic activity of p210 Bcr/Abl in differentiating myeloid progenitor cells. *Blood.* 2003;102(13):4547-4554.
41. Dror N, Alter-Koltunoff M, Azriel A, et al. Identification of IRF-8 and IRF-1 target genes in activated macrophages. *Mol Immunol.* 2007;44(4):338-346.
42. Huang W, Horvath E, Eklund EA. PU.1, interferon regulatory factor (IRF) 2, and the interferon consensus sequence-binding protein (ICSBP/IRF8) cooperate to activate NF1 transcription in differentiating myeloid cells. *J Biol Chem.* 2007;282(9):6629-6643.
43. Masumi A, Tamaoki S, Wang IM, Ozato K, Komuro K. IRF-8/ICSBP and IRF-1 cooperatively stimulate mouse IL-12 promoter activity in macrophages. *FEBS Lett.* 2002;531(12):348-353.
44. Eklund EA, Jalava A, Kakar R. PU.1, interferon regulatory factor 1, and interferon consensus sequence-binding protein cooperate to increase gp91(phox) expression. *J Biol Chem.* 1998;273(22):13957-13965.
45. Marecki S, Riendeau CJ, Liang MD, Fenton MJ. PU.1 and multiple IFN regulatory factor proteins synergize to mediate transcriptional activation of the human IL-1 beta gene. *J Immunol.* 2001;166(11):6829-6838.
46. Meraro D, Hashmueli S, Koren B, et al. Protein-protein and DNA-protein interactions affect the activity of lymphoid-specific IFN regulatory factors. *J Immunol.* 1999;163(12):6468-6478.
47. Rehli M, Poltorak A, Schwarzfischer L, Krause SW, Andreesen R, Beutler B. PU.1 and interferon consensus sequence-binding protein regulate the myeloid expression of the human Toll-like receptor 4 gene. *J Biol Chem.* 2000;275(13):9773-9781.
48. Unlu S, Kumar A, Waterman WR, et al. Phosphorylation of IRF8 in a pre-associated complex with Spi-1/PU.1 and non-phosphorylated Stat1 is critical for LPS induction of the IL1B gene. *Mol Immunol.* 2007;44(13):3364-3379.
49. DeKoter RP, Kamath MB, Houston IB. Analysis of concentration-dependent functions of PU.1 in hematopoiesis using mouse models. *Blood Cells Mol Dis.* 2007;39(3):316-320.